

# Dynamic changes of RNA-sequencing expression for precision medicine: N-of-1-pathways Mahalanobis distance within pathways of single subjects predicts breast cancer survival

A. Grant Schissler<sup>1,2,3,4,\*</sup>, Vincent Gardeux<sup>1,3,4,\*</sup>, Qike Li<sup>1,2,3,4,\*</sup>, Ikbel Achour<sup>1,3,\*</sup>, Haiquan Li<sup>1,3,4</sup>, Walter W. Piegorsch<sup>1,3,4,§</sup>, Yves A. Lussier<sup>1,2,3,4,§</sup>

<sup>1</sup>University of Arizona Center for Biomedical Informatics and Biostatistics (CB2), Tucson, AZ, USA

<sup>2</sup>Graduate Interdisciplinary Program in Statistics, University of Arizona, Tucson, AZ, USA

<sup>3</sup>Department of Medicine, University of Arizona, Tucson, AZ, USA

<sup>4</sup>BIO5 Institute, University of Arizona, Tucson, AZ, USA

\* Equal contribution, § Corresponding authors

## ABSTRACT

**Motivation:** The conventional approach to personalized medicine relies on molecular data analytics across multiple patients. The path to precision medicine lies with molecular data analytics that can discover interpretable single-subject signals (N-of-1). We developed a global framework, N-of-1-pathways, for a mechanistic-anchored approach to single-subject gene expression data analysis. We previously employed a metric that could prioritize the statistical significance of a deregulated pathway in single subjects, however, it lacked in quantitative interpretability (e.g., the equivalent to a gene expression fold-change).

**Results:** In this study, we extend our previous approach with the application of statistical Mahalanobis distance to quantify personal pathway-level deregulation. We demonstrate that this approach, N-of-1-pathways Paired Samples Mahalanobis Distance (N-OF-1-PATHWAYS-MD), detects deregulated pathways (empirical simulations), while not inflating false positive rate using a study with biological replicates. Finally, we establish that N-OF-1-PATHWAYS-MD scores are, biologically significant, clinically relevant, and are predictive of breast cancer survival ( $p < 0.05$ ,  $n = 80$  invasive carcinoma; TCGA RNA-sequences).

**Conclusion:** N-of-1-pathways MD provides a practical approach towards precision medicine. The method generates the magnitude and the biological significance of personal deregulated pathways results derived solely from the patient's transcriptome. These pathways offer the opportunities for deriving clinically actionable decisions that have the potential to complement the clinical interpretability of personal polymorphisms obtained from DNA acquired or inherited polymorphisms and mutations. In addition, it offers an opportunity for applicability to diseases in which DNA changes may not be relevant, and thus expand the "interpretable 'omics'" of single subjects (e.g. personalome).

**Availability:** <http://www.lussierlab.net/publications/N-of-1-pathways>

**Contact:** yves@email.arizona.edu

## 1 INTRODUCTION

Through the incorporation of molecular data into the patient care process, personalized medicine is drastically changing the healthcare landscape; however, truly precise medicine has not been obtained. Since completion of the human genome in 2003, the inclusion of molecular data in medicine has improved our ability to make accurate diagnoses, prognoses, and treatment plans. Relying

on large cohorts limits the application of many of these techniques, however. While inherited or acquired DNA polymorphisms provide powerful insight in the pathogenicity of many Mendelian diseases and in cancer, a single-subject interpretation of the transcriptome may provide insight and could be deployed in diseases incurred by other insults than DNA damage or inheritable defects. Conventional transcriptome analyses rely on multiple patient data that can mask idiosyncratic signals from a single patient, and these approaches may lead to treatments only effective for the "average" patient. Gene-level expression signatures found in cross patient studies do not adequately inform treatment plans for all cancer patients; therefore, there is a need for better methods to understand the biological underpinning at the single patient level.

In response to these issues, we developed a global computational framework: N-of-1-pathways. N-of-1-pathways is founded upon three principles: (1) single patient data represent the entire statistical universe, (2) significance and interpretation are derived from genesets (pathways), and (3) pathway level information is used to answer questions of clinical importance. Principle 1 allows for detection of individual signals that traditional cohort-level studies can overlook. Principle 2 anchors the results in mechanism and this affords dimension reduction and interpretation. Principle 3 provides quantitative and qualitative measures to address questions relating to patient care. The first application of the N-of-1-pathways framework, the N-of-1-pathways-Wilcoxon method (Gardeux, et al., 2014), successfully predicted lung adenocarcinoma patient outcomes using paired (normal and tumor) RNA-Seq samples from a single subject. A follow-up study established it could accurately identify experimentally deregulated pathway in ovarian and breast cancer cell lines (Gardeux, et al. 2014). While the N-of-1-pathways-Wilcoxon identified deregulated pathways with a statistical relevant, it did not quantify the magnitude of deregulation.

In this study, we extend and refine the N-of-1-pathways framework by developing a novel application of Mahalanobis Distance (MD) to create a "clinical relevance metric," providing insight on the magnitude of the deregulation in addition to the biological significance. The design of N-of-1-pathways MD eliminates the former's reliance on ranks (e.g. Wilcoxon test), while producing a measure of effect that is interpretable on the biological scale. We employ breast cancer gene expression data to show increased sensitivity while not increasing false positives in compari-

son to the Wilcoxon approach. Finally, we utilize the clinical relevance metric to predict breast cancer survival.

## 2 METHODS

### 2.1 Datasets and preprocessing

We used two datasets pertaining to breast cancer. Dataset I (GEO, GSE51403; (Liu, et al., 2014) allow us to assess false positive and negative rate. Dataset II was used in a validation study (Table 1). RNA-Seq counts of Dataset II were adjusted for ambiguous read assignment using the RSEM (RNA-Seq by Expectation Maximization) software (Gautier, et al., 2004; Li and Dewey, 2011). All measurements for both datasets were taken as base-2 logarithms ( $\log_2$ ) in the course of normalization. If several probes were mapped to the same HGNC gene name, the maximum expression value was retained as the gene expression value and considered for further analysis (Povey, et al., 2001).

**Table 1.** Datasets.

| Dataset Description | I Biological replicate study                                   | II Validation Study               |
|---------------------|--|-----------------------------------|
| Aim                 | 1. Assess false positive rate<br>2. Assess false negative rate | 1. Predict breast cancer survival |
| Authors             | Liu Y, Zhou J, White KP.                                       | NA                                |
| Source              | GEO, GSE51403  | TCGA_BRCA                         |
| Disease             | Breast Adenocarcinoma  | Breast carcinoma                  |
| Data Download Date  | Jan 2014   | Dec 2014                          |
| Data Type           | RNA-Seq  | RNA-Seq                           |
| Genomic Platform    | Illumina HiSeq 2000  | Illumina RNA-Seq V.2              |
| Genes Measured      | 22 336   | 20 501                            |
| Samples             | MCF-7 Cell line  | 80 Normal/Tumor <sup>‡</sup>      |
| Age Median (Range)  | NA   | 54 (30-90)                        |
| Disease Stage I     | NA   | 17 (21.3%)                        |
| Disease Stage II    | NA   | 40 (50.0%)                        |
| Disease Stage III   | NA   | 20 (25.0%)                        |
| Disease Stage IV    | NA   | 2 (1.25%)                         |

<sup>‡</sup> There were 112 original paired samples, reduced to 80 after applying the exclusion criteria (Methods 2.2)

### 2.2 TCGA\_BRCA Patient Exclusion Criteria

Out of the 112 breast cancer patients with paired normal/tumor samples in TCGA\_BRCA, 80 were considered for the validation analysis in this study. Patients were excluded from the study (i) who died of non-cancer causes in the first 12 months (defined as ‘tumor-free’ or ‘unknown tumor recurrence status’), (ii) who are living tumor-free with a clinical follow-up less than 12 months (not enough time to assess recurrence risk), and (iii) if male (only 1 such occurrence).

### 2.3 Geneset definitions and Gene Ontology annotations of Biological Processes (GO-BP)

We aggregated genes into genesets (pathway) using the Gene Ontology Biological Process, GO-BP (Ashburner, et al., 2000; Gene Ontology, 2010). Hierarchical GO terms were retrieved using the *org.Hs.eg.db* package of *Bioconductor* (Gentleman, et al., 2004) available for R (R Development Core Team, 2011) statistical software. We used the *org.Hs.egGO2ALLEGS* database (downloaded on 03/15/2013), which contains a list of genes annotated to that

GO term (*geneset*) along with all of its child nodes according the hierarchical ontology structure.

### 2.4 N-of-1-pathways Mahalanobis Distance: Producing a Clinical Relevance Metric (CRM)

N-of-1-pathways Mahalanobis Distance (MD) method consists of three core steps from input to output that were performed. Fig. 1 illustrates an overview of the method.

#### 1. Geneset (pathway) definition

For any given geneset, the paired expression values were restricted to only the genes within the pathway (Fig. 1A). To afford meaningful biological interpretation, genesets with at least 15 and no more than 500 genes were used in this study.

#### 2. Measure of deregulation and generation of the CRM

Pathway-level deregulation measurement is illustrated in Fig. 1B. All calculations involve only the expression of genes within the pathway. Genes were indexed within a given pathway by  $j=1, \dots, m$  and the  $\log_2$ -transformed normal and tumor expression values were denoted as  $N_j$  and  $T_j$ , respectively. For each gene, we considered no differential expression as the case where  $T_j = N_j$ . As shown in Fig. 1B, the diagonal line  $T_j = N_j$  provides a reference for calculation in quantifying differential gene expression. Then, for each  $j$ th gene we computed the signed Mahalanobis distance (Mahalanobis, 1936),  $d_j$ , from the point  $(N_j, T_j)$  to the diagonal line  $T_j = N_j$ . This is based on the distance from the point  $(N_j, T_j)$  to the point on the diagonal line of equal expression,  $(N_j, N_j)$ . Let the difference between the two points be the vector  $\Delta x$ :

$$\Delta x = (N_j, T_j) - (N_j, N_j) = (0, T_j - N_j). \quad (1)$$

Also let the bivariate sample’s variance-covariance matrix be:

$$\hat{\Sigma} = \begin{pmatrix} S_N^2 & S_{NT} \\ S_{TN} & S_T^2 \end{pmatrix}, \quad (2)$$

Where  $S_N$  is the sample standard deviation of the  $N_j$ s,  $S_T$  is the sample standard deviation of the  $T_j$ s, and  $S_{TN} = S_{NT}$  is their sample covariance.

Now, denote the reciprocal of the variance-covariance matrix’s determinant as:

$$\delta = \frac{1}{S_N^2 S_T^2 - (S_{NT})^2}. \quad (3)$$

By definition, the squared, vertical, Mahalanobis distance (MD) for gene  $j$  is the quadratic form

$$\begin{aligned} d_j^2 &= (\Delta x)^T \hat{\Sigma}^{-1} \Delta x \\ &= \delta \begin{pmatrix} 0 & T_j - N_j \end{pmatrix} \begin{pmatrix} S_T^2 & -S_{NT} \\ -S_{TN} & S_N^2 \end{pmatrix} \begin{pmatrix} 0 \\ T_j - N_j \end{pmatrix} \\ &= \delta (T_j - N_j)^2 S_N^2 \quad (S_{NT} = S_{TN}) \\ &= \frac{S_N^2}{S_N^2 S_T^2 - (S_{NT})^2} (T_j - N_j)^2 \quad (\text{using 3}). \end{aligned} \quad (4)$$

Then, the signed distance is

$$d_j = \sqrt{\frac{S_N^2}{S_N^2 S_T^2 - (S_{NT})^2}} (T_j - N_j) \quad (5)$$

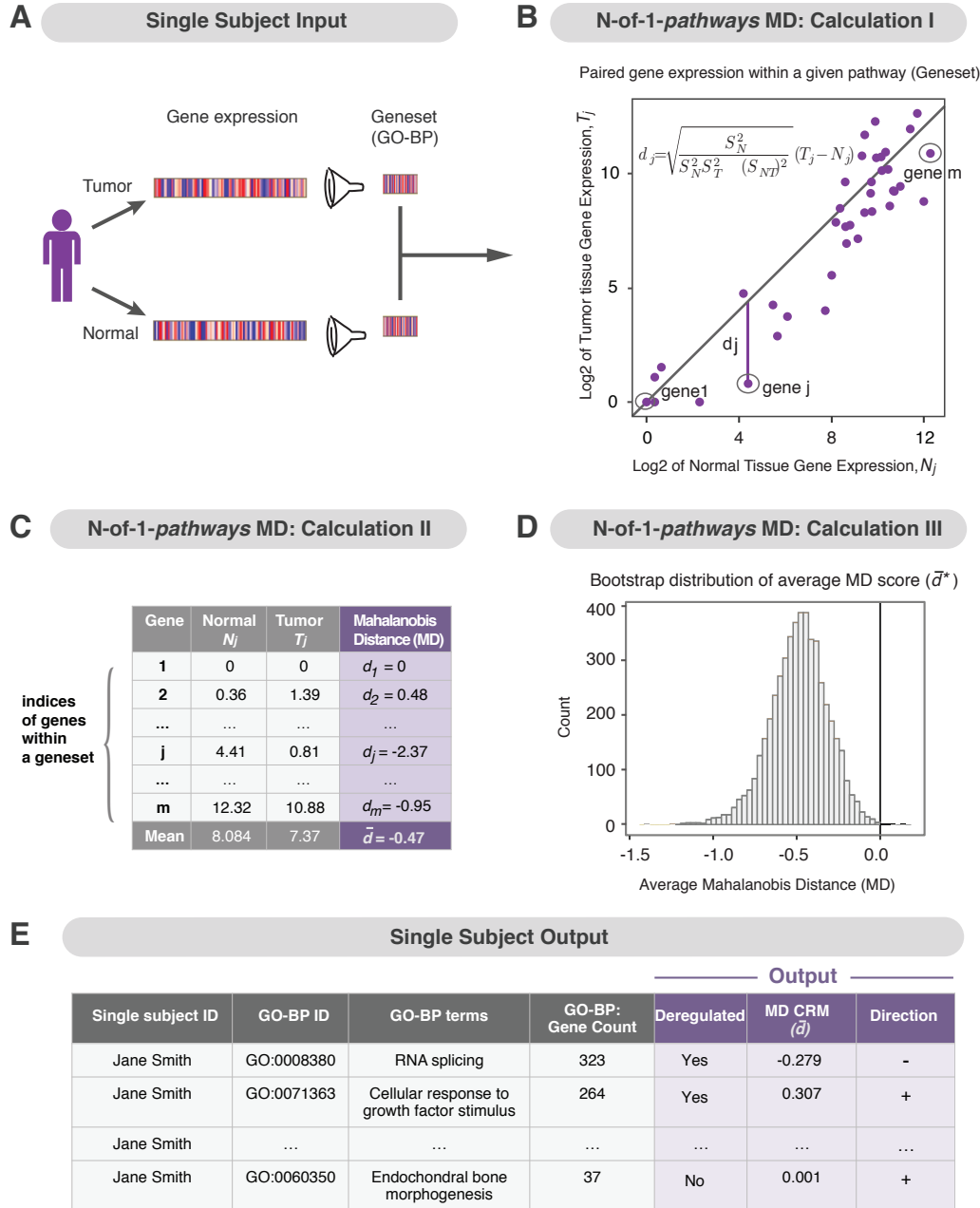


**Fig. 1. Method Overview of N-of-1-pathways Mahalanobis Distance.** (A) The input is represented by the gene expression of single patient paired samples (e.g. tumor vs normal tissue) filtered into *a priori* defined genesets (e.g. Gene Ontology Biological Processes: GO-BP pathways). (B) Calculation I is visualized by the bivariate relationship between normal and tumor gene expression values for a given geneset (e.g. GO-BP pathway). The vertical, signed Mahalanobis distance (MD),  $d_j$ , is computed from each  $j$ th point (gene) to the diagonal line representing equal expression. (C) Calculation II: The mean MD represents the pathway-level deregulation from normal to tumor expression where a negative value indicates down-regulation and a positive value represents up-regulation. The gene indices are randomly resampled and the “average MD score” is re-computed via bootstrapping (Chernick, 2008) to determine pathways with strong evidence of deregulation. (D) Calculation III: The bootstrap distribution of “average MD scores”. (E) The process results in pathway-level quantification of deregulation, an approach to obtain a Clinically Relevant Metric.

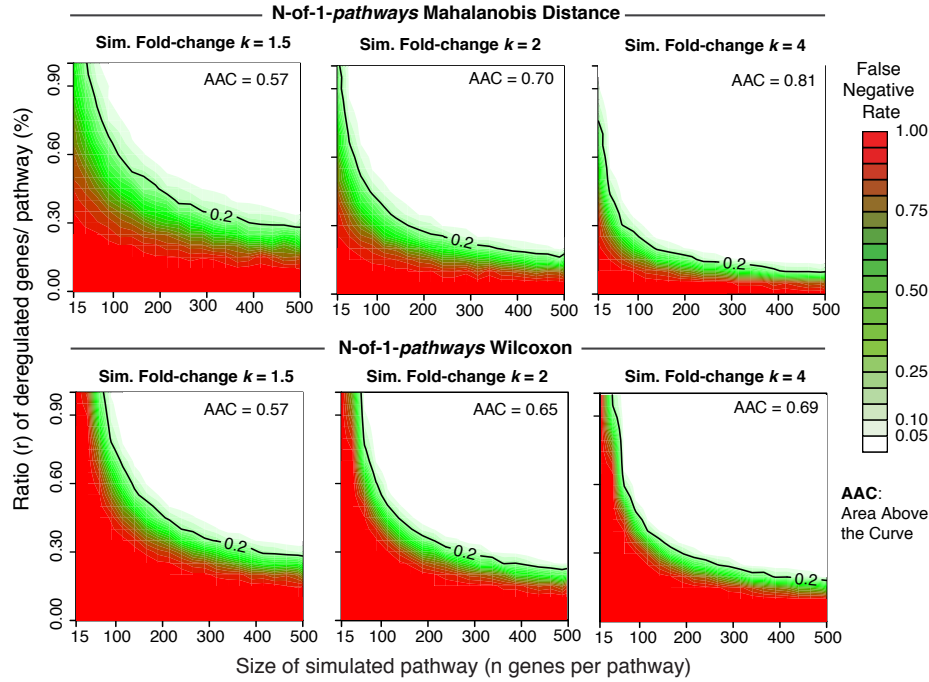


**Fig 2. Simulation study reveals that N-of-1-pathways MD powerfully detects artificially deregulated pathways.** Each point represents one size of a simulated pathway generated by randomly selecting  $n$  genes and a ratio  $r$  of the deregulated genes within the pathway (Table 1 Dataset 1, Methods 2.6). The ratio  $r$  is artificially increased by a  $k$ -fold change in a simulated pathway generated from biological replicates, ( $k = 1.5, 2, 4$ ). We then applied separately the N-of-1-pathways-Wilcoxon (bottom) and N-of-1-pathways-MD (top) methods to identify whether the truly deregulated pathway is detected. We repeated the process 5000 times at each combination of ( $n, k, r$ ) to estimate the false negative error rate (Wilcoxon p-values were Bonferroni adjusted with a 1% threshold). AAC, Area Above the Curve, quantifies the proportion of simulated pathway combinations with false negative error less than 0.20 (the black curve labeled 0.20 is the reference for this measure). Higher AAC indicates a greater number of scenarios with at least 80% power to detect deregulated pathways. N-of-1-pathways-MD outperforms N-of-1-pathways-Wilcoxon at every fold-change, requiring fewer genes in the pathway and a smaller ratio of deregulated genes. Notably, the simulated false positive rate (0.0% deregulated genes; rate along the horizontal axis) is smaller for MD than Wilcoxon, averaging 0.14% and 0.94%, respectively. This rate can also be interpreted as the simulated rate of discovery when two non-tumor samples are paired. **Legend**, Sim. = simulated, AAC=area above curve

The sign is taken to indicate the direction of deregulation: down- or up-regulated pathway. Note that when the signed distance is simple Euclidean distance it is a **log<sub>2</sub> fold change**. We opted to employ the Mahalanobis distance, which from the derivation above is seen to be a form of adjusted **distance that accounts for the variance-covariance structure of the paired samples**.

Finally, after each  $d_j$  is determined, we computed the un-weighted average of the distances,  $\bar{d}$ , to provide a geneset-level summary statistic of deregulation. This average is the CRM of pathway deregulation, the mean MD score:

$$\bar{d} = \sum_{j=1}^m d_j / m. \quad (6) \text{ (CRM)}$$

### 3. Assess certainty of the CRM via bootstrapping

To accumulate evidence that any observed difference is truly representative of differential geneset deregulation, a bootstrap distribution for  $\bar{d}$  is calculated (Chernick, 2008). This is conducted by randomly sampling with replacement indices from the geneset under study and calculating a new, bootstrapped  $\bar{d}^*$ . Fig. 1C shows the measurements for a given pathway and indicates the gene indices for resampling. Fig. 1D depicts a bootstrap distribution and marks the  $d = 0$  reference line at which no deregulation occurs. Fig. 1E represents an example of an MD score,  $\bar{d}$ , for each pathway, along with its pathway description and direction of deregulation.

Based on the bootstrap resample, we identify a pathway as deregulated if the bootstrap distribution of  $\bar{d}^*$  separates completely from  $d = 0$ . That is, if all its  $\bar{d}^*$ s lie to a single side of the  $d = 0$  reference line, either up-regulated ( $\bar{d} > 0$ ) or down-regulated ( $\bar{d} < 0$ ). To set the number of bootstrap resamples, we imitated a technique often seen in multiple testing: we employed at least  $1/\alpha_j$  resamples, where  $\alpha_j$  is a Sidak-adjusted  $\alpha$ -level for comparing  $J$  pathways at a pointwise level of  $\alpha = 0.01$ . This is  $1/\alpha_j = 1/(1 - (1 - \alpha)^{1/J}) = 1/(1 - (0.99)^{1/J})$ . For a prototypical collection of, say,  $J = 5000$  pathways, this gives  $1/(1 - (0.99)^{1/J}) > 497\,496.3$ , so we operated with 500 000 bootstrap resamples. Using 500 000 bootstrap resamples, at least 8 genes in the pathway are recommended as to not frequently resample the same finite possibilities (since  $7^7 < 500\,000$ ).

### 2.5 Simulation study: assessing false negative rate

To assess false negative rate of the N-of-1-pathways MD method, we performed a simulation study by creating synthetic genesets that contain a percentage of concordant (all up) deregulated genes using Dataset 1 (biological replicates of breast cancer cell lines). The intent is to simulate deregulated pathways as described in our previous work (Gardeux, et al., 2014) with some modifications. For each gene, we assumed a negative binomial distribution and estimated the mean and overdispersion parameters from the seven biological replicates via the method of moments. Under our pa-

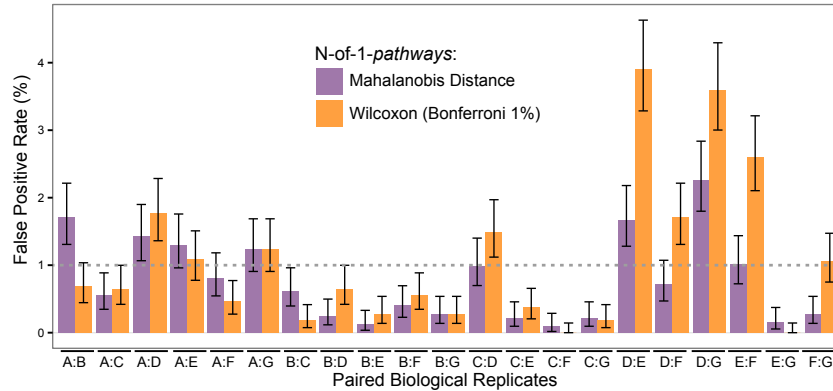


**Fig. 3. Evaluation of the false positive rate of N-of-1-pathways MD compared to the Wilcoxon method.** Pairs of biological replicates from breast cancer cell lines were used (Table 1 dataset III). 3228 GO-BP genesets were tested for each pair of biological replicates to find falsely deregulated pathways using both the N-of-1-pathways MD and Wilcoxon methods (Wilcoxon p-values are Bonferroni adjusted and a 1% threshold is applied). Thin black lines are 95% pointwise Agresti-Coull intervals for the proportion of false positives; bar heights are the percentage of falsely identified deregulated pathways. N-of-1-pathways MD performs equally or better than Wilcoxon. Technical replicates showed similar results using GEO20194 (data not shown).

rameterization, a negative overdispersion parameter indicates underdispersion for a gene, which is anticonservative. Thus when underdispersion occurs, we conservatively assumed that the variance equals the mean for that gene. For a fixed set of simulation settings ( $n$ =genes in pathway,  $r$ =ratio of deregulated genes in pathway,  $k$ =fold change), we produced two synthetic “normal” transcriptomes (two realizations for each of the 22 336 genes measured). We then produced one artificially deregulated transcriptome by multiplying the gene mean by  $k$ . Then a geneset of size  $n$  genes was randomly selected with that genewise adjusted location parameter. We randomly indexed a subset of size  $r$  from that geneset to retrieve the artificially deregulated transcriptome. The remaining  $n - r$  genes were selected from the second normal transcriptome. We combined these two genes to create a synthetic “tumor” sample of size  $n$  with the correct amount of deregulation. We completed the synthetic pathway of paired gene expression by selecting the appropriate genes from the first normal transcriptome. At each combination of  $(n, k, r)$ , N-of-1-pathways MD and Wilcoxon methods were executed 5000 times (implemented in R, using the University of Arizona Extremely LarGe Advanced Technology, ‘El Gato,’ computing system) (Fig. 2). For the Wilcoxon method, a pathway is found deregulated when the Bonferroni adjusted p-value  $< 0.01$ . The proportion of times the pathway is not detected as deregulated is the simulated false negative error rate.

## 2.6 Biological replication study: assessing false positive rate

We assess the false positive rate of the N-of-1-pathways MD method via the biological replication study. We paired biological replicates and identified GO-BP terms as deregulated using N-of-1-pathways methodology. Agresti-Coull confidence intervals (Brown, et al., 2001) for the proportion of deregulated pathways found in each sample in Dataset I were computed using the *binom* package in R. If an interval had a lower bound less than 0, the lower bound was replaced with 0 (Fig. 3). R package *ggplot2* was used for visualization (Wickham, 2009).

## 2.7 Principal component analysis of CRM

Principal component analysis (PCA) (Jolliffe, 2005) was executed on the N-of-1-pathways MD pathway scores using the *prcomp* function from the *stats* package in R. The PCA was performed using scores from GO-BP terms that were found deregulated in at least one of the 80 patients in Dataset II (validation study); 2130 GO-BP terms were selected.

## 2.8 Partitioning around medoids clustering of CRMs

Unsupervised clustering (Witten and Frank, 2005) of pathway scores for the 2130 GO-BP terms found deregulated in at least one of the 80 breast cancer patients (Dataset II) was performed using the Partitioning Around Medoids (PAM) method (Kaufman and Rousseeuw, 1990) (via the *cluster* package in R) (Fig. 4).

## 2.9 Kaplan-Meier survival curve

Kaplan-Meier survival curves (Kleinbaum and Klein, 2005) were computed via GraphPad Prism V.6.02 software using the survival data associated with the breast cancer validation dataset (Dataset II); see Fig. 4. PAM-derived clusters were used to distinguish the two survival curves (see Methods 2.8).

## 2.10 Star Plots of Diametric Extreme Patients

Star plots were computed in R using the *stars* function in the default *graphics* package (Fig. 5: Panel C). The stars plots display 15 pathways chosen to discriminate between the patients who are Disease-Free Survival (DFS) longer than 4 years and the patients who suffer Death of Disease (DoD) in less than 2.5 years. The pathways were selected by retaining the top largest absolute two-sample  $t$  statistic for each GO-BP term. Once the pathways were chosen, each patient has an individual star plot where each edge represents a particular GO-BP MD CRM. In order to have a relevant representation of the star plot surface, a biologist manually curated the pathways to a representative GO-BP category as shown in Fig. 5: Panel B.

### 2.11 N-of-1 Diametric Extreme Paired Analysis and comparison to GSEA, DEG + Enrichment

Using the diametric extreme phenotypes (Fig 5) we produced all 45 possible combinations of Disease-Free Survival > 4 years patients (DFS, n=9) with Death of Disease < 2.5 years patients (DoD, n=5). We applied the N-of-1-pathways MD framework to these pairs of subjects in pursuit of phenotypically deregulated pathways. To test against a conventional approach, we identified differentially expressed genes (DEGs) using the full cohort of diametric extremes via *EBseq* R package following the suggested protocol (Leng, et al., 2013). Then we performed geneset enrichment with those DEGs using Fisher's Exact Test (FET) to quantify the association of DEG status vs. pathway inclusion. We also applied standard GSEA on the diametric extreme patients to detect deregulated GO-BP terms (Subramanian, et al., 2005). To validate the results, we compared the detected pathways with an independent gold standard (GS) of 11 GO-BP terms determined through network models of ten breast cancer survival studies (Chen, et al., 2010). We summarize the overlap and functional similarity between detected pathways from the three methods and the GS in Table 3. Functional similarity between GO-BP was determined at a conservative cutoff of 0.7 using information theoretic similarity (ITS) methods we previously validated (Gardeux, et al., 2014; Gardeux, et al., 2014; Li, et al., 2012; Regan, et al., 2012; Tao, et al., 2007).

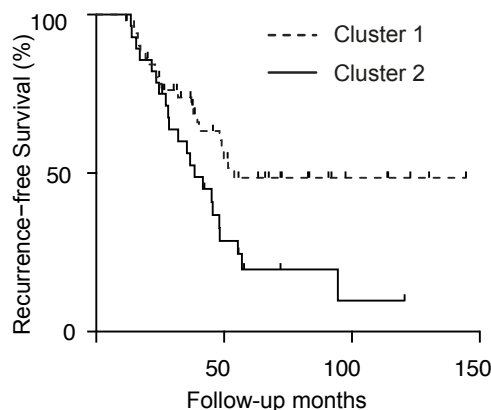


**Fig. 4. N-of-1-pathways MD GO-BP clinical importance metrics predict breast cancer patient survival.** N-of-1-pathways MD was applied to n=80 invasive breast carcinoma patients (TCGA\_BRCA, RNA-seq, Table 1 dataset II) resulting in 3225 clinical importance metrics. Every patient has an N-of-1-pathways MD score for each of the identified deregulated pathways (2130 pathways identified in at least one patient) and we performed principal component analysis and unsupervised clustering on these scores. As shown in the figure, unsupervised Partitioning around medoids (PAM) clustering reveals distinct Kaplan-Meier survival curves (log-rank test p-value < 0.05). Additionally, the identified pathways can be also used to discover a fully specified classifier for good vs. poor prognosis (Supp. Table S5). Reducing dimensionality further, we constructed the clusters based on only the top 10 scored pathways and produced distinct survival curves (Supp. Fig. S7). When compared to gene expression, N-of-1-pathways performed similarly (Supp. Fig. S1). We found that pathway-level scores relate to pathologically determined stage (Wilcoxon p-value between 1<sup>st</sup> principal component of MD Score = 0.02; data not shown), but did not identify receptor subtypes (ns; principal components 1-5 verified; data not shown)

## 3 RESULTS

### 3.1 N-of-1-pathways Mahalanobis Distance identifies synthetically deregulated pathways

We aimed to assess false negative rates by designing a simulation study using the RNA-Seq gene expression from biological replicates of breast cancer cell lines (Dataset I). We extend our previous simulation study by parametrically modeling RNA-seq counts using the negative binomial distribution. We employ this simulation to evaluate the predictive power of our N-of-1-pathways MD method (Gardeux, et al., 2014). The N-of-1-pathways MD method is consistently more powerful than Wilcoxon. Fig. 2 shows that both methods perform better as the pathway size and number of deregulated genes increases. We quantify the scenarios that achieve greater than 80% power (less than 20% false negative rate) by measuring the Area Above the Curve (AAC). We note that N-of-1-pathways MD outperforms the Wilcoxon method at every fold-change studied.

### 3.2 N-of-1-pathways Mahalanobis Distance slightly outperforms Wilcoxon in false positive rate

We evaluated the false positive rate of the N-of-1-pathways MD compared to its Wilcoxon counterpart (Fig. 3). To this end, we used Dataset I of 7 biological replicates from a breast cancer cell line. The rationale adopted was that biological replicates derived from the same breast cancer cell line should lead to similar gene expression profiles with minimal variation and, therefore, any genesets found deregulated could be labeled as a false positive.

### 3.3 N-of-1-pathways MD predicts breast cancer survival

While breast cancer is often effectively treated, it is known for high heterogeneity and predicting clinical outcomes remains a challenge. We sought out to predict breast cancer survival using the N-of-1-pathways MD scores from 80 women with paired RNA-Seq gene expression samples (Tumor and Normal) (Table 1; Methods section 2.7). We observed large variation in the number of deregulated pathways found. Using the MD CRM, the number of identified deregulated pathways per patient ranged from 19 to 970 when screening 3225 GO-BP terms (average of 278 pathways per patient). The most commonly deregulated pathways across patients were related to cell division and cell cycle, known to be associated to cancer pathology (Table 2). As a negative control, we investigated the distribution of MD CRMs from pathways not identified in any of the patients. We found that the 1095 unidentified pathway MD CRMs did not produce distinct Kaplan-Meier survival curves (log-rank p-value=0.133; data not shown). Delving deeper into the N-of-1-pathways MD scores, we performed a principal component analysis (PCA) to distinguish diametric extreme patients (Supp. Fig. S4). We first identified all pathways that were found deregulated in at least one patient. This allowed for no individualized deregulation signal to be overlooked when determining cohort-level trends. There were 2130 selected GO-BP terms using this criterion; every patient has a CRM for each of these pathways. The first component of these pathway scores did not differ between the diametric extreme patients (Wilcoxon p-value > 0.2). We then performed unsupervised clustering of the same N-of-1-pathways MD scores to predict survival among the 80 breast cancer patients.



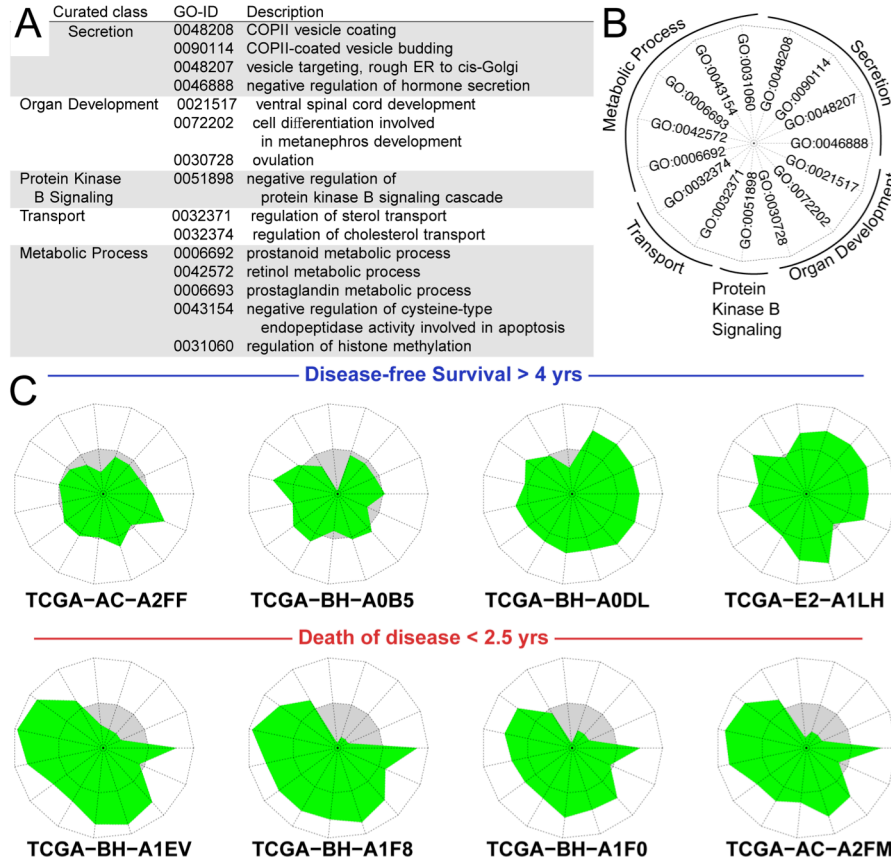


**Fig. 5. N-of-1-pathways representation (star plot) of individual GO-BPs of diametric extreme patients.** The top 15 most discriminating GO-BP terms were identified between the two groups of patients with diametric extreme phenotype (death of disease in less than 2.5 years,  $n=5$ ; at least 4 years of disease-free survival,  $n=9$ ; **Methods 2.10**). **Panel A** shows GO terms manually curated to interpretable categories. **Panel B** provides the legend of the star plots, each edge corresponding to one GO term, each star reflects a single patient's deregulation as measured by the MD CRM for each pathway. **Panel C** contains a sample of eight patients' star plots (four from each extreme). The white zone represents up-regulated pathways (given the N-of-1-pathways direction of deregulation), while the grey zone stands for down-regulation. The circle separating the grey and white areas represents non-deregulation (MD CRM = 0).

We used Partitioning around Medoids (PAM) clustering with two medoids to produce two clusters of patients. The two clusters of patients showed a statistically significant difference in survival (log-rank test  $p$ -value < 0.05; **Fig. 4**). Additionally, vital status was associated with the clusters (Fisher's exact test  $p$ -value < 0.01; data not shown).

**Table 2.** Most commonly deregulated breast cancer pathways among the 80 patients.

| GO-BP ID   | GO-BP Terms                           | Patient Count |
|------------|---------------------------------------|---------------|
| GO:0000236 | mitotic prometaphase                  | 65            |
| GO:0000216 | M/G1 transition of mitotic cell cycle | 57            |
| GO:0000280 | nuclear division                      | 57            |
| GO:0048285 | organelle fission                     | 57            |
| GO:0007059 | chromosome segregation                | 56            |
| GO:0000087 | M phase of mitotic cell cycle         | 56            |
| GO:0003012 | muscle system process                 | 55            |
| GO:0007067 | mitosis                               | 55            |
| GO:0000075 | cell cycle checkpoint                 | 54            |
| GO:0006936 | muscle contraction                    | 54            |

Our exploration of the diametric extremes yields two key observations. The star plots display distinct, interpretable signals for Death of Disease less than 2.5 years (**Fig 5**) while the pattern for Disease-Free Survival greater than 4 years remains ambiguous. Secondly, N-of-1-pathways finds phenotypic differences using only one subject per group. The pairing of diametric extremes resulted in 45 applications of N-of-1-pathways. The number of detected pathways ranged from 36 to 756 for the diametrically opposed pairs, averaging 161 pathways per pair. **Table 3** presents the most relevant pathways.

On the other hand, traditional geneset approaches were underpowered in this setting. Differentially expressed genes (DEGs) analysis (Leng, et al., 2013) required an FDR adjusted  $p$ -value less than of 20% to find 65 genes differentially expressed genes across the diametric extreme cohort ( $n=14$ ). The following geneset enrichment found only one pathway enriched at Fisher's Exact Test FDR adjusted  $p$ -value < 0.1. 17 pathways were found enriched at FDR 25%. None of these pathways were related to the gold standard. GSEA yields only 4 pathways at FDR 25%, and none of these pathways were related to our breast cancer gold standard (Subramanian, et al., 2005).

**Table 3. N-of-1-pathways MD identifies phenotypically deregulated pathways when conventional methods fail.** Using the diametric extreme phenotypes (Fig 5) we produced all 45 possible pairs of disease-free survival > 4 years patients (DFS, n=9) with death of disease < 2.5 years patients (DoD, n=5). Within these pairs of diametrically opposed patients, the gene-level log<sub>2</sub> fold change centered around zero, indicating no systematic shift in expression. We applied the N-of-1-pathways framework to these pairs in pursuit of phenotypically deregulated pathways. Displayed are the pathways detected most often (found deregulated at least 25 times) in the 45 pairs that also share functional information similarity with an independent gold standard (GS) of 11 GO-BP terms (Methods 2.11, (Chen, et al., 2010). Every patient studied was deregulation in this pathway (i.e., not just a few patients causing deregulation in pairs). Note that DEG + geneset enrichment and GSEA using all 14 diametric extreme patients detected 18 and 4 pathways, respectively (FDR 25%); none of these pathways were functionally related to the GS.

| GO ID   | Description                 | Number of<br>Detections | Patient Count<br>DFS DoD |
|---------|-----------------------------|-------------------------|--------------------------|
| 0000280 | nuclear division**          | 31                      | 9 5                      |
| 0048285 | organelle fission**         | 31                      | 9 5                      |
| 0007067 | mitosis*                    | 30                      | 9 5                      |
| 0000236 | mitotic prometaphase**      | 28                      | 9 5                      |
| 0051301 | cell division*              | 27                      | 9 5                      |
| 0007017 | microtubule-based process** | 26                      | 9 5                      |
| 0016568 | chromatin modification**    | 26                      | 9 5                      |

\* Pathway was found in the gold standard. \*\* Pathway shared > 0.7 ITS with a pathway in the gold standard.

## 4 DISCUSSION

Rank-based, non-parametric approaches can suffer a decreased efficiency compared to appropriately implemented bootstrap, randomization, and t-test procedures (Smucker, et al., 2007). Further, the Wilcoxon procedure we previously utilized assumes that the pairs are chosen randomly and independently from a population. It is presumable that gene expression values do not satisfy this assumption. We aimed to address these concerns via an evolution of our approach into the N-of-1-pathways Mahalanobis Distance method. Results from our exploration of TCGA breast cancer data show N-of-1-pathways MD improves upon our earlier N-of-1-pathways Wilcoxon approach. The success of the N-of-1-pathways framework for breast cancer builds upon the insights developed in our previous investigation of TCGA lung adenocarcinoma data (Gardeux, et al., 2014), as TCGA data share similarity in data generation, storage, and format, as well as other aspects. N-of-1-pathways MD continues to maintain the practicality of self-contained geneset testing (Goeman and Bühlmann, 2007). Additionally, the method provides a pathway-level deregulation clinically relevant metric that is predictive of clinical endpoints.

Our simulation study of the method's ability to detect synthetically deregulated pathways indicates that N-of-1-pathways MD outperforms N-of-1-pathways Wilcoxon. Its ability to identify entire mechanistically interpretable pathways deregulated from subtly differentially expressed genes is very powerful. This feature provides a strategy to assess the notion that complex diseases may derive from multiple changes of small effect that lead to larger phenotypic outcomes. Furthermore, we note the signed nature of the N-of-1-pathways MD score that the method cannot detect deregulated pathways that are not primarily up- or down-regulated. In other words, if a pathway has approximately equal numbers of

genes above and below the line of equal expression, N-of-1-pathways MD would likely not identify the pathway as deregulated. It is debatable whether such a specific form of departure reflects true deregulation or simply a highly variable pathway.

Our biological replicate analysis indicates N-of-1-pathways MD produces slightly fewer false positives than Wilcoxon. There may be some concern over the somewhat inflated rate of false positives for certain samples. This might be attributed to true pathway deregulation explained by measurement variability or some aspect of the replication that led to unequal distribution of mRNA molecules. We note that this analysis is highly contingent on proper preprocessing and normalization. Normalization is particularly problematic in RNA-seq as many normalization techniques fail to compensate for library size, gene length, and guanine-cytosine content (Dillies, et al., 2013). Notably, N-of-1-pathways did not exhibit a bias towards longer median length of their genes (Supp. Figure S3, Panel A), nor higher gene intensities within the pathway (Supp. Figure S3, Panel B). However, there is a bias towards detecting larger pathways as deregulated (Supp. Figure S3, Panels C-D).

Applying N-of-1-pathways MD to breast cancer data results in the discovery of sensible deregulated pathways and produces metrics predictive of survival. This aspect validates the notion that N-of-1-pathways MD not only provides a metric interpretable at the pathway level, but also is related to important clinical endpoints. The most commonly deregulated pathways (Table 2) are associated with the hallmarks of cancer, including deregulation in DNA replication and cell cycle. We also utilized the principal components of the MD CRMs (Methods 2.6) to identify clinical subtypes such as estrogen receptor (ER)+ and clinical metastatic stage. The former is not significant (Wilcoxon p-value > 0.08; PC1, data not shown); the latter is significant (Wilcoxon p-value < 0.05; PC1, data not shown). Additionally, the breast cancer findings strengthen our previous indication that N-of-1-pathways was predictive of lung adenocarcinoma survival, demonstrating the robustness of our techniques for different cancer types.

Survival prediction is possible from tumor gene expression alone (Supp. Fig S1), but the gene signatures may lack interpretability and clinically actionable targets. N-of-1-pathways is designed to first discover deregulated pathways at the individual subject level followed by learning classifiers cross-subjects. In contrast, gene expression classifiers work directly on gene expression, which may not be functionally deregulated at the individual subject level as pointed out by Simon (Simon, 2005). N-of-1-pathways also allows for more power in discovering group comparisons at the pathway level that traditional differential mRNA expression followed by enrichment studies as summarized by Table 3.

N-of-1-pathways MD refines our Wilcoxon approach. We acknowledged in our previous work that independence assumptions of the N-of-1-pathways Wilcoxon signed-rank test were not met. However, the fact that a predictive and interpretable signal was captured gave credibility to the N-of-1-pathways approach. N-of-1-pathways MD improves over our previous work as it does not violate any such statistical foundations. Careful readers may note that we have avoided the notions of hypothesis testing and prefer the term “identified pathways” to “significantly deregulated pathways.” The MD-deregulation criterion outlined in Methods 2.4.3 provides a metric to identify an up- or down-regulated pathway, but does not rely on the notion of a p-value. We do retain the p-



values and associated multiplicity corrections for the Wilcoxon approach, in order to faithfully replicate that methodology. Further study is required to create a statistically complete approach.

The introduction of N-of-1-pathways MD provides many avenues for extension. The method can be adapted to more than paired samples. Multiple samples could be obtained from within a tumor and the pathway scores would measure intratumor heterogeneity. Along the same vein, multiple samples could be obtained from a patient over time. Thus, the geneset scores would measure longitudinal change in key pathways to predict response to therapy or to make timely prescriptive decisions. Additionally, the N-of-1-pathways framework could potentially provide a basis for improved small sample normalization techniques. Or, additional ontological information could be employed to weight genes within a pathway and reflect gene importance in biochemical dynamics. It remains to be shown whether the patient-specific deregulated pathway(s) identified in the current study can be predictive and it will be addressed in future studies. N-of-1-pathways can also be applied to various scales of biology, e.g. DNA, methylation patterns, or microRNA expression.

## 5 CONCLUSION

We hypothesized that creating a biologically relevant pathway-level measure of effect will improve interpretability and detection while maintaining statistical precision. We have established a novel application of statistical Mahalanobis distance, N-of-1-pathways MD, to quantify geneset deregulation using gene expression data from paired samples derived from a single subject. This study further validated our N-of-1-pathway framework by predicting breast cancer survival from the pathway-level metric of deregulation. We evaluated the precision and accuracy of N-of-1-pathways MD and compared it to our existing Wilcoxon approach. We found improvement in geneset deregulation detection while not suffering increased false positive rates.

The modification of our approach is a pathway-level approach to produce a clinical relevance metric (CRM) in single subjects and quantifying the deregulation induced under the disease condition (e.g. tumor sample) for each pathway (Shriner, et al., 2014). In addition, we are currently evaluating prospectively the method to predict future hospitalization in a clinical trial.

N-of-1-pathways MD provides a practical approach towards precision medicine. The method gives clinically actionable results derived solely from the patient. The entire transcriptome does not need to be measured, allowing for targeted experiments across multiple gene expression platforms, reducing cost and providing flexibility. The method generates the magnitude and the biological significance of personal deregulated pathways results derived solely from the patient's transcriptome. These pathways offer an opportunity for applicability to diseases in which DNA changes may not be relevant, and thus expand the "interpretable 'omics'" of single subjects (e.g. personalome).

## ACKNOWLEDGEMENTS

We greatly appreciate the support of Ms. Colleen Kenost and Dr. Nima Pouladi. An allocation of computer time from the UA High

Performance Computing (HPC) and High Throughput Computing (HTC) at the University of Arizona is gratefully acknowledged.

**Funding:** This study was supported in part by The University of Arizona Cancer Center, The University of Arizona BIO5 Institute, The University of Arizona Center for Biomedical Informatics and Biostatistics, and the University of Arizona Health Sciences Center. This material is based upon work supported by the National Science Foundation under Grant No. 1228509.

## REFERENCES

- Ashburner, M., et al. Gene ontology: tool for the unification of biology. The Gene Ontology Consortium. *Nat Genet* 2000;25(1):25-29.
- Brown, L.D., Cai, T.T. and DasGupta, A. Interval estimation for a binomial proportion. *Statistical Science* 2001:101-117.
- Chen, J., et al. Protein interaction network underpins concordant prognosis among heterogeneous breast cancer signatures. *Journal of biomedical informatics* 2010;43(3):385-396.
- Dillies, M.-A., et al. A comprehensive evaluation of normalization methods for Illumina high-throughput RNA sequencing data analysis. *Briefings in bioinformatics* 2013;14(6):671-683.
- Gardeux, V., et al. 'N-of-1-pathways' unveils personal deregulated mechanisms from a single pair of RNA-Seq samples: towards precision medicine. *Journal of the American Medical Informatics Association : JAMIA* 2014;21(6):1015-1025.
- Gardeux, V., et al. Concordance of deregulated mechanisms unveiled in underpowered experiments: PTBP1 knockdown case study. *BMC medical genomics* 2014;7 Suppl 1(Suppl 1):S1-S1.
- Gautier, L., et al. affy-analysis of Affymetrix GeneChip data at the probe level. *Bioinformatics (Oxford, England)* 2004;20(3):307-315.
- Gene Ontology, C. The Gene Ontology in 2010: extensions and refinements. *Nucleic Acids Res* 2010;38(Database issue):D331-335.
- Gentleman, R.C., et al. Bioconductor : open software development for computational biology and bioinformatics. *Genome biology* 2004(10).
- Goeman, J.J. and Bühlmann, P. Analyzing gene expression data in terms of gene sets: methodological issues. *Bioinformatics (Oxford, England)* 2007;23(8):980-987.
- Jolliffe, I. Principal component analysis. Wiley Online Library; 2005.
- Kaufman, L. and Rousseeuw, P.J. Partitioning around medoids (program pam). *Finding groups in data: an introduction to cluster analysis* 1990:68-125.
- Leng, N., et al. EBSeq: an empirical Bayes hierarchical model for inference in RNA-seq experiments (vol 29, pg 1035, 2013). *Bioinformatics* 2013;29(16):2073-2073.
- Li, B. and Dewey, C.N. RSEM: accurate transcript quantification from RNA-Seq data with or without a reference genome. *BMC bioinformatics* 2011;12:323-323.
- Li, H., et al. Complex-disease networks of trait-associated single-nucleotide polymorphisms (SNPs) unveiled by information theory. *J Am Med Inform Assoc* 2012;19(2):295-305.
- Liu, Y., Zhou, J. and White, K.P. RNA-seq differential expression studies: more sequence or more replication? *Bioinformatics* 2014;30(3):301-304.
- Mahalanobis, P.C. On the generalized distance in statistics. *Proceedings of the National Institute of Sciences (Calcutta)* 1936;2:49-55.
- Povey, S., et al. The HUGO Gene Nomenclature Committee (HGNC). *Human genetics* 2001;109(6):678-680.
- R Development Core Team, R. 2011. R: A Language and Environment for Statistical Computing. Release 2.11.1.
- Regan, K., et al. Translating Mendelian and complex inheritance of Alzheimer's disease genes for predicting unique personal genome variants. *J Am Med Inform Assoc* 2012;19(2):306-316.
- Shriner, D., Adeyemo, A. and Rotimi, C.N. Reconciling clinical importance and statistical significance. *European journal of human genetics : EJHG* 2014;22(2):158-159.
- Simon, R. Roadmap for developing and validating therapeutically relevant genomic classifiers. *J Clin Oncol* 2005;23(29):7332-7341.
- Smucker, M.D., Allan, J. and Carterette, B. A comparison of statistical significance tests for information retrieval evaluation. In, *Proceedings of the sixteenth ACM conference on Conference on information and knowledge management*. Lisbon, Portugal: ACM; 2007. p. 623-632.
- Subramanian, A., et al. Gene set enrichment analysis: a knowledge-based approach for interpreting genome-wide expression profiles. *Proc Natl Acad Sci U S A* 2005;102(43):15545-15550.
- Tao, Y., et al. Information theory applied to the sparse gene ontology annotation network to predict novel gene function. *Bioinformatics* 2007;23(13):i529-538.
- Wickham, H. ggplot2: Elegant Graphics for Data Analysis. Springer; 2009.
- Witten, I.H. and Frank, E. Data Mining: Practical machine learning tools and techniques. Morgan Kaufmann; 2005.